Journal of Low Temperature Physics, Vol. 134, Nos. 1/2, January 2004 (© 2004)

Time-of-Flight Measurements on Quantized Vortex Lines in Rotating ^{3}He-B

A.P. Finne*, V.B. Eltsov*†, R. Blaauwgeers*‡, Z. Janu*§, M. Krusius*, L. Skrbek*§

* *Low Temperature Laboratory, Helsinki University of Technology, Finland*
† *Kapitza Institute for Physical Problems, Kosygina 2, 119334 Moscow, Russia*
‡ *Kamerlingh Onnes Laboratory, University of Leiden, Holland*
§ *Joint Low Temperature Laboratory, Institute of Physics ASCR and Charles University, V Holešovičkách 2, 180 00 Prague, Czech Republic*

Vortex loops are injected into a long cylindrical sample of rotating vortex-free superfluid ^{3}He-B. Using non-invasive NMR techniques, we measure the time required for them to expand along the sample axis to form rectilinear vortex lines. From the axial flight time we deduce the dissipative mutual friction parameter α which is found to agree with previously reported measurements. The flight time displays no anomaly at $0.6T_c$, where the character of the vortex dynamics abruptly changes from regular over-damped flow to turbulence.

PACS numbers: 67.40.Vs, 47.32.Cc.

Among the coherent quantum systems superfluid ^{3}He-B is a special case: Owing to the large variation in hydrodynamic properties with temperature and pressure, the formation and dynamics of quantized vortices display novel phenomena. In rotating ^{3}He-B high-velocity vortex-free superflow can be maintained in metastable conditions. Vortex loops can then be injected and their motional properties can be studied in two different flow regimes: (i) At high temperatures ($T > 0.6\,T_c$) friction is large, vortex motion is overdamped, and their number remains conserved. (ii) At low temperatures ($T < 0.6\,T_c$) friction approaches zero, Kelvin wave excitations are weakly damped and propagate along the vortices, which leads to loop formation, reconnections, and rapidly proliferating turbulence.[1] Here we report on flight-time measurements of vortex propagation along the rotation axis when vortex seed loops are injected into vortex-free rotation.

In ^{3}He superfluids the normal component is highly viscous. In these measurements it can be considered immobile in the rotating frame ($\mathbf{v}_n = 0$). When vortex loops are injected into vortex-free superflow at constant rota-

0022-2291/04/0100-0375/0 © 2004 Plenum Publishing Corporation

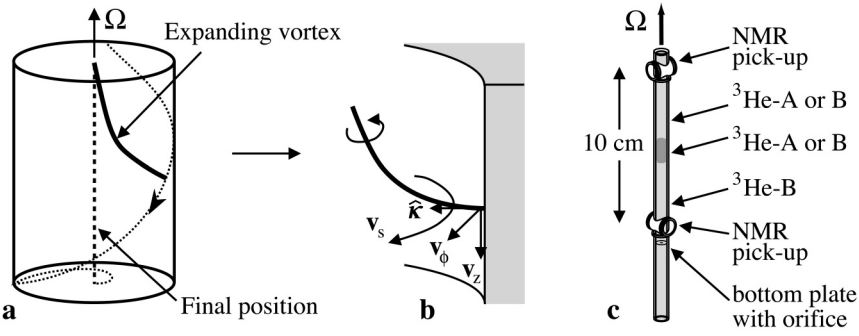

Fig. 1. a) Trajectory of the end point of an injected vortex loop on the cylindrical sample boundary and b) the velocity components governing its motion. c) The sample volume is contained within an 11 cm long smooth-walled tube of $R = 3\,\mathrm{mm}$ radius. It is closed off with a bottom plate which includes a central orifice of 0.5 or 0.7 mm diameter for thermal contact to the liquid column below and the refrigerator.

tion Ω, they undergo a transient expansion into rectilinear vortices, which then are stable in time at temperatures above $0.4\,T_c$. The expansion is governed by the balance between the Magnus force from the superflow $\mathbf{v}_s = \mathbf{\Omega}\times\mathbf{r}$ and the mutual friction force from the coupling to normal excitations. In the rotating frame with $\mathbf{v}_n = 0$, the vortex velocity $\mathbf{v}$ is given by

$$\mathbf{v} = \mathbf{v}_s - \alpha'\hat{\boldsymbol{\kappa}} \times [\mathbf{v}_s \times \hat{\boldsymbol{\kappa}}] + \alpha[\mathbf{v}_s \times \hat{\boldsymbol{\kappa}}], \tag{1}$$

where $\hat{\boldsymbol{\kappa}}$ is a unit vector in the direction of the vortex line while α and α' are the dissipative and reactive mutual friction parameters.

At the end point of a vortex which slides on the cylindrical side wall of the sample (Fig. 1b) $\hat{\boldsymbol{\kappa}}$ is oriented perpendicular to the wall, and $v_s = \Omega R$. From Eq. (1) we find that the vertical component of vortex motion at its end $v_z = \alpha v_s$ measures the dissipative mutual friction, while the azimuthal component $v_\phi = (1-\alpha')v_s$ gives the reactive part. The axial flight time τ_F of the end point over a vertical distance d is $\tau_F = d/(\alpha\Omega R)$. In the limit of weak surface pinning and high flow velocity $\mathbf{v}_s$, the propagation of a vortex along the sample is fastest at its end and the vorticity at smaller radii $r < R$ lags behind.

Our rotating ^{3}He-B sample (Fig. 1c) is monitored with two independent cw NMR spectrometers which have their pick-up coils at the top and bottom ends of the sample cylinder.[2] A sudden change in the NMR absorption spectrum signals the arrival of the vorticity into the volume within the coil with a resolution which is better than one rectilinear vortex above $0.8\,T_c$ and

still better than 10 lines at $0.4\,T_c$. A magnetic barrier field of up to 0.5 T can be applied to the center section of the sample, to stabilize the ^{3}He-A phase. At pressures $p < 21$ bar, two AB interfaces then separate a layer of ^{3}He-A of variable height from long sections of ^{3}He-B above and below. At higher pressures there may be one or two AB interfaces, depending on prehistory.[3] Our measurements have been performed at 10.2, 29.0, and 33.7 bar pressure in the temperature interval 0.45-0.95 T_c.

To measure a flight time τ_F, which corresponds to a known distance d, the simplest alternative is to have a burst of vorticity leaking through the orifice,[4] which is located at the bottom of the sample volume (Fig. 1c). Here the barrier field should be zero so that the sample volume is filled with only ^{3}He-B. One then records the time difference between the moments when vorticity is first detected in the two NMR coils. This process is observed below $0.60\,T_c$. Since there is some ambiguity in how to confirm the orifice leak as the source for the detected vorticity, we describe a second measurement first which involves the AB interface instability.

When an AB interface exists in the middle of the sample (Fig. 1c), it undergoes at a critical superflow velocity a Kelvin-Helmholtz shear-flow instability. A small number of vortex loops is ejected in such an event from the A to the B phase.[3,5] During a slow increase of Ω the event is first seen at a rotation velocity which we call Ω_c^*. It depends on temperature (T), pressure (p), and the profile $H_b(z)$ of the barrier field. When these variables are kept constant and Ω is slowly ramped up, $\Omega(t) = \dot{\Omega}t$, we find Ω_c^* to be reproducible to within 1 %. After the instability a few vortex loops end up protruding across the AB interface to the B phase side, with one end of the loops on the cylindrical side wall and the other perpendicular to the AB interface in the center of the cylinder. The loops then start their expansion towards the NMR pick-up coil. The distance d of the AB interface is determined from the calculated field profile $H_b(z)$ of the barrier solenoid.[6] Since Ω is still increasing while the loops expand, the measured apparent critical velocity Ω_c^*, at which the vortices reach the coil, is different from the true Ω_c:

$$\Omega_c^{*2} = \Omega_c^2 + 2\frac{d}{\alpha R}\dot{\Omega}. \tag{2}$$

Thus a measurement of Ω_c^* as a function of the rotational acceleration $\dot{\Omega}$ gives both the true Ω_c of the KH instability and the vortex damping α (Fig. 2).

At low pressures with two AB interfaces each measurement gives two values of Ω_c and α. These correspond to vortex motion upward and downward from the two AB interfaces in Fig. 1c. The magnetic profile $H_b(z)$ is sufficiently symmetric such that the same Ω_c is measured for the top and bottom sections within our precision (Fig. 3). The same applies for the extracted α values. Thus for now we leave it open whether the injection events

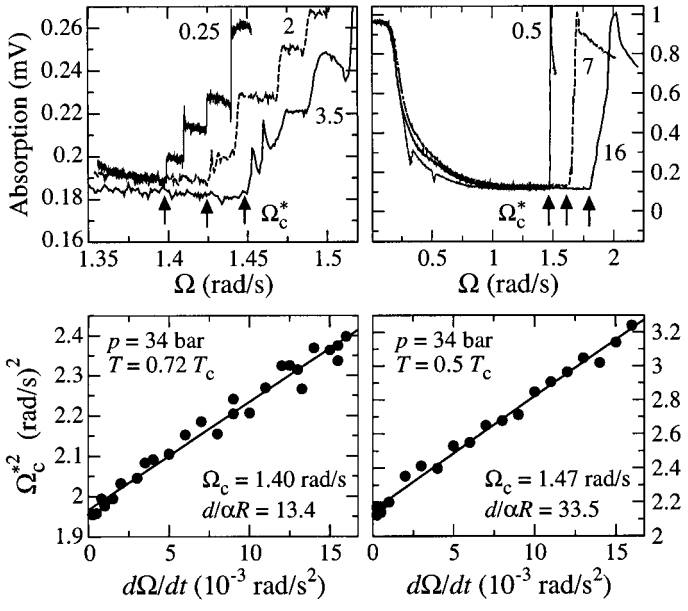

Fig. 2. Measurement of vortex loop expansion following the AB interface instability. *(Top)* a) Above $0.6\,T_c$, the instability occurs repeatedly as a function of Ω, as shown by the staircase-like increase in NMR absorption. The height of a step is proportional to the number of rectilinear vortices formed in the instability event. The labels on the NMR absorption traces refer to $\dot{\Omega}$ in units of 10^{-3} rad/s^2. b) Below $0.6\,T_c$, the instability is followed by turbulent loop expansion which fills the B phase with the equilibrium number of rectilinear vortices. Only one instability event is thus seen in the Ω range of the figure. The sudden massive rise of the NMR absorption signal at Ω_c^* is followed by slow relaxation which represents the rarefaction and polarization of the tangled vorticity into rectilinear lines.[1] *(Bottom)* Measurements of the apparent critical velocity Ω_c^* as a function of the rotational acceleration $\dot{\Omega}$ follow Eq. (2) both c) above and d) below $0.6\,T_c$. No discontinuity is observed in the temperature dependences of the extracted values of Ω_c and α at $0.6\,T_c$ (Fig. 3).

at the upper and lower AB interfaces are correlated or statistically independent. Our α values in Fig. 3 are in good agreement with earlier data from Ref. [7]. This is an interesting conclusion since the loop expansion process undergoes a sudden change from regular to turbulent behavior on cooling below $0.6\,T_c$.[1] As seen in Fig. 2a, above $0.6\,T_c$ only a few rectilinear vortex lines are formed in each KH instability event.[8] Below $0.6\,T_c$ the loops are un-

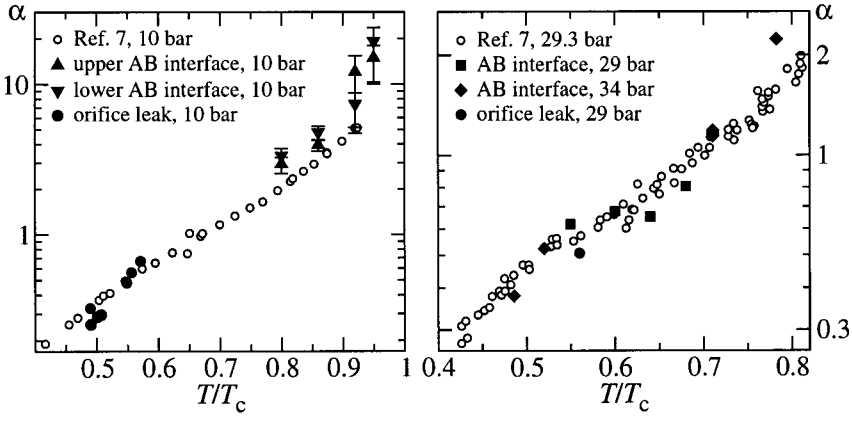

Fig. 3. Dissipative mutual friction coefficient α versus temperature at three different pressures. Our data (filled symbols) agree with Ref. 7.

stable with respect to further loop formation in the high-velocity superflow. Here the loop expansion process is transformed into full-blown turbulence which after one instability event fills the B phase with the equilibrium number of rectilinear vortex lines (with more than 10^3 vortex lines in the case of Fig. 2b).[1] In spite of this fundamental change in the motion of the vorticity along the sample, the flight time measurement does not distinguish between these two regimes of vortex dynamics. This becomes evident from a comparison of the two lower panels in Fig. 2. These record measurements above and below $0.6\,T_c$: The dependence of Ω_c^{*2} on $\dot{\Omega}$ remains linear in both cases and gives continuous well-behaved values for Ω_c and α. We take this to be evidence for the fact that the end point motion along the cylindrical wall entirely dominates in the axial penetration of the vorticity along the sample.

In the absence of an AB interface, B-phase vortex formation may be controlled by a few different processes, which have different temperature dependences.[9] The process with the lowest critical velocity $\Omega_c(T)$ at a given temperature T dominates. In the overlap regime, where the temperature dependences of two processes cross, one may find either process. Here it may be difficult to distinguish from where the injected vortices originate, but the present setup with two pick-up coils gives more information. Below $0.6\,T_c$ vortices in the orifice in the center of the bottom plate of the sample volume are easily displaced by noise in the rotation drive and a burst of vortex loops may be injected into the sample volume.[4] It then evolves into a turbulent tangle and ultimately fills the sample with the equilibrium number of vortices (Fig. 4). These events can be added into Fig. 3, since they correspond to a flight time over the maximum possible distance d, the separation between

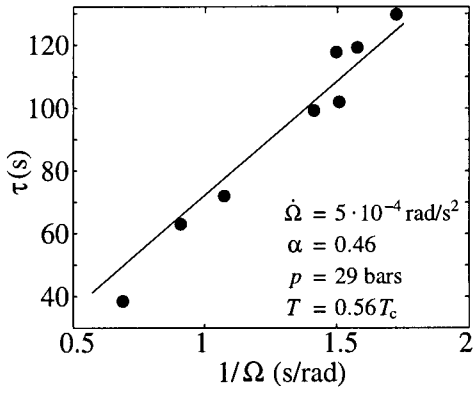

Fig. 4. Flight time of turbulent vortex propagation over the distance $d = 10\,\mathrm{cm}$ separating the two NMR coils in Fig. 1c, measured after a burst of vortex loops has leaked through the orifice into the sample volume at varying rotation velocities Ω. The slope of the fitted line $\tau_F = d/(\alpha\Omega R)$ gives α.

the two detector coils. Even if other sources of vortex formation should intervene, the leaks through the orifice provide the maximum envelope curve for $\tau_F(T)$.

To conclude, when quantized vorticity is injected at one end of a rotating initially vortex-free sample of ^{3}He-B, it propagates axially, pulled by the motion of the end points of vortex lines along the cylindrical wall. The border between vortex-free superflow and vorticity advances thus first along the wall. The velocity of this border is governed by the dissipative mutual friction at all temperatures above $0.4\,T_c$, both at low temperatures, where vortex motion is turbulent, and at high temperatures, where it is over-damped.

This work was supported in part by the following EU and ESF research programmes: EU-IHP ULTI-3, ESF-COSLAB, ESF-VORTEX. LS wishes to thank for the grant GAČR (202/02/0251) and ZJ for GAČR 102/02/0994.

REFERENCES

1. A.P. Finne *et al.*, *Nature* **424**, 1022 (2003).
2. R. Blaauwgeers *et al.*, *Physica B* **329-333**, 93 (2003).
3. R. Blaauwgeers *et al.*, *Phys. Rev. Lett.* **89**, 155301 (2002).
4. L. Skrbek *et al.*, *Physica B* **329-333**, 106 (2003).
5. R. Blaauwgeers *et al.*, *Physica B* **329-333**, 57 (2003).
6. V.B. Eltsov *et al.*, *Physica B* **329-333**, 96 (2003).
7. T.D.C. Bevan *et al.*, *J. Low Temp. Phys.* **109**, 423 (1997).
8. R. Hänninen *et al.*, *Phys. Rev. Lett.* **90**, 225301 (2003).
9. V.M.H. Ruutu *et al.*, *J. Low Temp. Phys.* **107**, 93 (1997).